Int. J. Electrochem. Sci., 10 **(2015)** 5624 - 5638

International Journal of
ELECTROCHEMICAL
SCIENCE
www.electrochemsci.org

Influence of Electrochemical Treatment over Cellular Adherence onto the Surface of Titanium Surgical Implants

Adrian Voicu, Narcis Duţeanu, Aurel Răduţă, Nicolae Vaszilcsin[*]

Universitatea Politehnica Timişoara, 300006 Piata Victoriei 2, Timişoara, Romania,
[*]E-mail: nicolae.vaszilcsin@upt.romailto:jpshim@kunsan.ac.kr

Received: 15 December 2014 / *Accepted:* 2 May 2015 / *Published:* 27 May 2015

In the present paper, a correlation between the anodizing potential, morphology and thickness of the titanium oxide surfaces formed on Ti as well as the roughness and adhesion degree of mesenchymal cells onto such functionalized surfaces are analysed. Experiments were performed using 20 mm × 10 mm × 1.5 mm Ti plates cut by electroerosion. After chemical polishing in a mixture containing HF, HNO_3 and H_2SO_4 and then passivation in a solution of 10% HNO_3, Ti plates were anodized in a 1 mol L^{-1} H_3PO_4 solution at a voltage between 40 and 250 V. In all experiments, the anodizing time was 1 minute. The surface morphology of anodized Ti plates was characterized by optical and scanning electron microscopy. As expected, the average thickness of the anodized layer is strongly dependent on the anodizing voltage. Thicknesses ranging between 3.1 (40 V) and 12.6 μm (250 V) were obtained. The surface roughness values of the anodized Ti plates ranged between 0.575 (anodizing voltage of 40 V) and 0.998 (250 V), whereas the surface roughness of the untreated plate was 0.489. These values are large enough to ensure good cellular adherence onto Ti implants. The corrosion tests indicate that mass losses in Ringer lactate standard solution have values up to 3 μm, which is acceptable in such conditions. Mesenchymal trypsinized cells were used to evaluate the cell adhesion degree. By analysing the results, we concluded that to obtain a maximum degree of cell adhesion, the optimal ratio between anodization and cellular adherence occurs at 150 V.

Keywords: Corrosion, Titanium anodizing, Cellular adherence, Titanium implant, Surgical implant.

1. INTRODUCTION

The considerable increase in human life expectancy is reflected somehow by the accelerated growth in the use of implants and medical devices that are in contact with body tissues [1, 2]. Metals, such as Ti and its alloys, are preferred as biomaterials due to their excellent biocompatibility, chemical

stability and mechanical properties. In pure form, Ti does not have all the properties required by different types of implants currently used in traumatology and orthopaedics.

Growth, proliferation and differentiation of mesenchymal stem cells (MSCs) onto the surface of surgical implants may be the solution for the tissue integration of these implants [3, 4]. Unfortunately, the method is limited by the low level of adhesion of MSCs onto metal surfaces. A possible solution to the poor adhesion is prior functionalization of the surfaces.

All of the relevant research results to date definitively demonstrate the fact that Ti is an osteoinductor biomaterial, in other words, the osteocytes adhere directly onto its surface, unlike other materials used for surgical implants manufacturing, for which osteointegration is achieved through an intermediary layer of fibrous tissue. Therefore, the qualities and corrosion resistance of the Ti oxide thickness on the surface of the implants significantly influence cellular adherence, thereby influencing the biocompatibility of Ti [3, 5].

Surface energy, texture, layer thickness, roughness and other surface characteristics of a biomedical implant can significantly influence the interaction of the implant with the surrounding biological / biochemical environment [5, 6]. Among all parameters of implants surface, the easiest to be measured and with a direct influence on cellular adherence are layer thickness, corrosion rate and surface roughness [3, 7, 8].

Electrochemical anodization is a well-known method used for the preparation of TiO_2 thin films [9, 10, 11]. The structure, morphology and properties of titanium oxide layers vary with anodizing parameters, such as oxidation potentials, oxidation time, film growth patterns and film growth rates. The electrolytic solution also proved to play a key role on the formation and crystallization of anodic titanium oxides. Usually, for biomedical purposes, the use of simulated body fluids (SBFs) at 37° is recommended [12, 13].

The aim of the present study is to determine a value of the anodizing potential for which an optimum relation is obtained between the corrosion rate and the extent of cell adhesion, which is very important for some medical applications involving tissue integration of the implant [2, 3].

2. EXPERIMENTAL

Experimental anodizing approach was made on CP Grade 2 Titanium plates of 20 mm × 10 mm × 1.5 mm that were cut using the DK7732F wire spark erosion machine. Subsequently, the plates were machined to remove the burr and round the edges and corners to avoid dendritic depositions in the area. Chemical polishing of the plates was performed afterwards using a mixture containing HF, HNO_3 and H_2SO_4. The next step consisted in their chemical passivation in a solution of 10% HNO_3, according to ASTM F86-04: Standard Practice for Surface Preparation and Marking of Metallic Surgical Implants [14]. All samples were then ultrasonically cleaned in deionized water.

The actual anodization process was performed in a 1 mol L^{-1} H_3PO_4 solution for 1 minute under potentiostatic conditions. The electrical parameters of the anodizing process are presented in Table 1.

The microstructures were analysed using an Olympus BX51M optical microscope and a stereo Olympus SZ7X microscope.

Table 1. Electrical parameters of the anodization process.

Experiment No.	Voltage [V]	Maximal current [A]
1	40	0.3
2	60	0.8
3	80	2.3
4	100	2.8
5	120	3.4
6	140	3.9
7	160	4.3
8	200	5.5
9	250	6

2.1. Electrochemical measurements

Cyclic voltammetry measurements using Voltalab 21 potentiostat and its own software Volta Master 4 were performed to determine the corrosion behaviour. Electrochemical cell BEC / EDI, made of Pyrex glass, allowing for thermostatic control, was used, equipped with a titanium working electrode, a platinum electrode B35M110 1 XM110 (Ø = 1 mm, l = 10 mm) and a calomel reference electrode B20B110 1 XR110 as a counter electrode. The corrosion tests were performed under environmental conditions close to physiological conditions: pH 7.3 to 7.4. For all samples, the test temperature was maintained at 37±0.2 °C using an ultra-thermostat. Ringer lactate was used as working solution because it acts as a BSF environment. Voltamograms were drawn at 50 mV s^{-1} (anodizing) and 1 mV s^{-1} for the corrosion Tafel slopes.

2.2. Surface roughness

The experimental measurements were made on seven standard reference lengths (7 × 0.8 mm = 5.6 mm), and the roughness parameters were determined according to DIN standards. The D and P profiles obtained for anodized samples were taken into consideration.

2.3. MSCs adherence

To test the degree of adhesion to the titanium surfaces previously functionalized via anodization, mesenchymal cells were used. These cells were trypsinized (isolated from the tissue with trypsin), counted, dosed, and then incubated in a culture medium, where titanium plates were also added. The method is based on the property of MSCs to adhere onto plastic surfaces and is the most commonly used method, due to the low cost and large amount of MSCs obtained compared to the other methods.

3. RESULTS AND DISCUSSION

3.1. Surface morphology

The metallographic analysis highlights the morphological changes on the surface of the plates, which exhibit different aspects depending on the applied potential. The initial structure of the analysed samples is composed of polyhedral grains of α-Ti, with their grain sizes corresponding to an 8-9 score. The characteristics of the anodized layer are shown in figures 1 a-i.

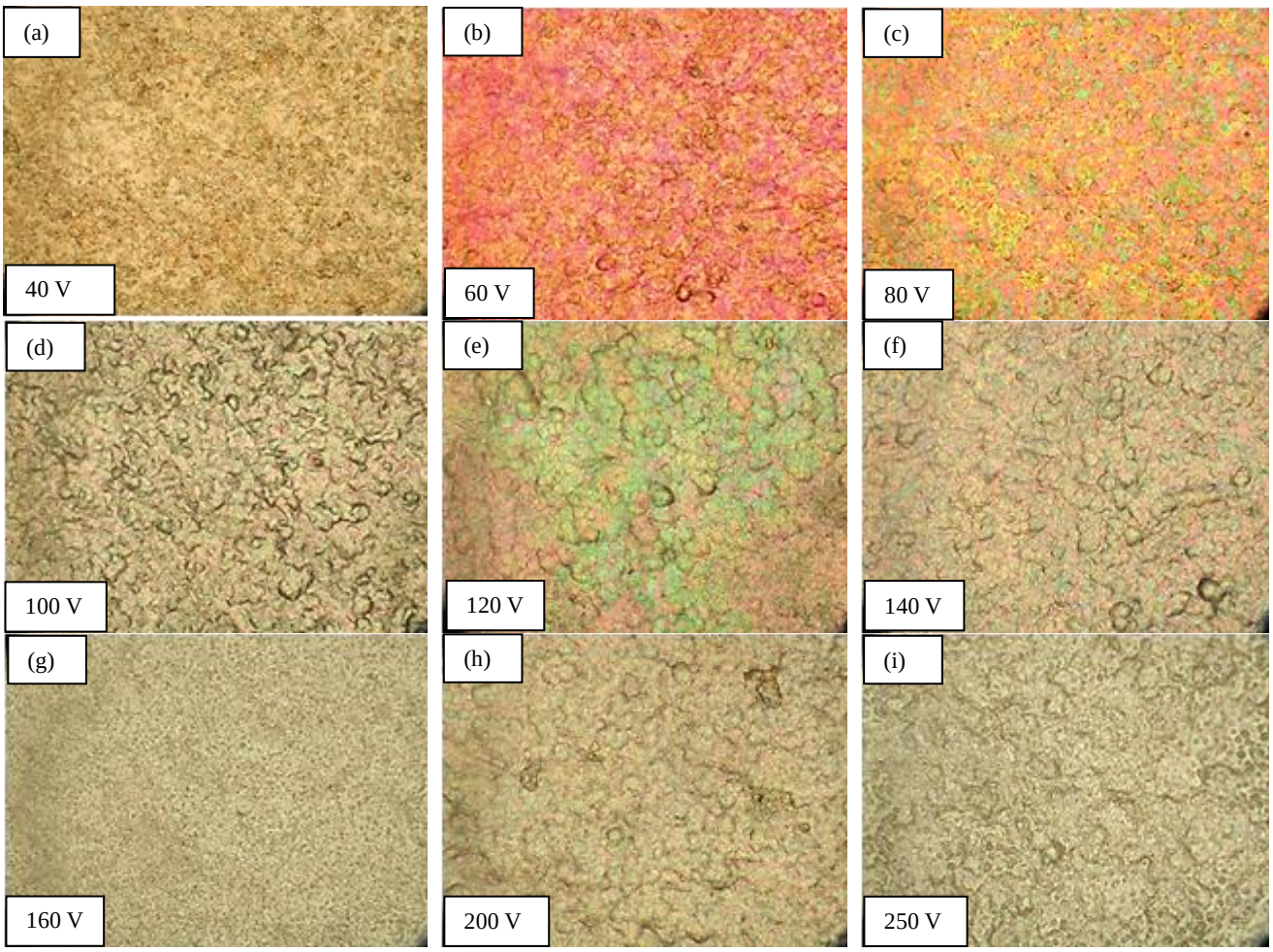

Figure 1. a-i: Microscopic structures of the samples anodized at 40 – 250 V; OM 500×.

The value of the potential of 40 V used for the first anodization process (figure 1a) is only slightly above the minimum breakdown value of the native oxide layer. The resultant changes in this case are minimal. After anodizing titanium at 60 V (figure 1b), visible changes on the surface of plates are begin to appear, with these exhibiting a pink-purple colour. The colour is due to the pores that are formed on the superficial titanium oxide surface acting as a diffraction grating. The colour varies (for all samples), depending on the characteristics of the incident light.

The 80 V (fig. 1c) anodization process produces an intensification of the colour, which has a bluish tint. An increase in the diameter of the pores is observed. Following a 100 V (figure 1d)

anodization process, the pores formed have larger dimensions than in previous situations, thus affecting the appearance of the surface. A grey colour that appears becomes enhanced with increasing applied voltage.

Increasing the applied voltage to 120 V (figure 1e) is accompanied by an increase in the pore diameter at the surface of the sample and a sharper grey tone.

For samples anodized at 140 V (figure 1f), the pore diameter increases and the grey tone becomes dominant.

For the applied voltage of 160 V, (figure 1g) the surface takes on a matte grey, evenly distributed appearance. The pore diameter is even larger than those of the lower applied voltages and begins to exhibit early damage due to lightning on the surface of the sample.

Another operating mode starts at 200 V (figure 1h). Simple anodization of the surface is replaced by MAO (Micro-Arc Oxidation). The same phenomenon was observed for the sample anodized at 250 V (figure 1). MAO induces a local melting of the sample and the appearance of micro-cracks.

Anodization and MAO are very similar techniques. The potential required for micro-arc oxidation is higher than for simple anodization, resulting in the generation of discharges/plasma. Electrical discharges start to occur on the surface of the sample in the form of micro-arcs that leave traces in the form of craters. The oxide layer surface is melted in this condition and replaced with a newly formatted one, with different aspect and properties. After MAO treatment, a porous titanium film was formed on the titanium surface with numerous opened micro-pores. The pore diameters varied from 2 to 9 μm. The holes in the surface are channels of micro-arc discharges in the electrolyte. The presence of micro-pores and cracks on the surface of MAO coatings can be considered to be an opportunity. The presence of a porous outer layer in MAO coatings would significantly improve the surface roughness and cellular adherence, resulting in higher bond strength [15, 16, 17, 18].

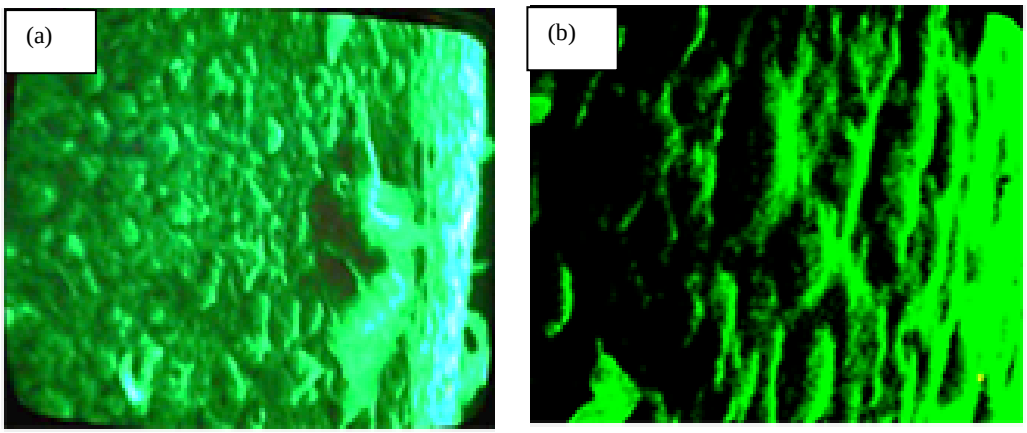

Figure 2. Scanning electron microscopy at 1800× (a) and 3000× (b) for the sample anodized at 250 V.

At 250 V (figure 1i), the frequency and density of electrical discharges on the surface further increase compared to the cases of the lower applied potentials. The number and depth of the craters on the surface of the sample increase accordingly. Spot melting occurs, which may cause an embedding of the ions of the electrolyte.

The surface condition for the sample anodized at 250 V was analysed using scanning electron microscopy at magnifications of 1800× (figure 2a) and 3000× (figure 2b). The results reveal an uneven surface, which is rough and has amorphous deposits caused by precipitation of electrolyte salts.

3.2. Layer thickness

The cross section of the anodized coating microstructure was metallographically analysed. Figures 3 a-i present the appearance of the surfaces of the samples and the corresponding anodized layer structures.

Polarized light microscopy and dark field illumination were used. The first signs of anodization appear in figure 3 a. As the applied voltage is only slightly above 37 V, the voltage limit necessary for the breakthrough of the TiO_2 dielectric layer that forms spontaneously, the changes are minimal; the newly formed oxide layer has a relatively variable thickness, with an average of only 3.11 μm. Note that this thickness, however minimal, is greater than the thickness of the layer formed spontaneously, which has values within the normal range of 20-40 nm. Changes occurred only on the surface of the sample and did not affect the structure of the substance.

Figure 3b shows that the average thickness of the anodized layer is 6 μm, but the layer is evenly distributed on the surface of the sample and has a more compact shape. The three-layered structure of the anodized layer begins to become visible. This phenomenon occurs because the anodization is a mass transport process. The Ti^{4+} ions migrate to the surface of the sample, whereas the ions of the electrolyte migrate in depth. The metal prevails in the deep layer, located directly on the sample surface; in the next layer, the metal oxide is present with an amount of electrolyte embedded in it; and the top layer has a higher content of electrolyte due to the titanium oxide ions. The titanium granular structure is not affected in this case. Figure 3c shows that the titanium oxide layer has an average thickness of approximately 6 μm, which is a good value compared with the other measurements. The oxide layer has a good adherence to the surface and a uniform thickness. The layer mainly containing the metal oxide has a greater thickness. Otherwise, the titanium metallographic structure remained unchanged.

For the sample anodized at 100 V, the average layer thickness is 5 μm. The appearance is uniform and adherent to the surface of the sample. The metallographic sample structure was not affected by the anodization process (figure 3d). For the sample anodized at 120 V (figure 3e), the average thickness of the layer is 6 μm, comparable to those previously obtained. Oxide surface layer, however, is more adherent and uniform. The metal was not affected at larger depths.

For the sample anodized at 140 V (figure 3f), the average thickness of the oxide layer was found to increase to a value of 8.5 μm. The ratio of the inner layer, containing predominantly oxides of titanium that are responsible for the proper grip, and the outer layer, with high electrolyte content that is responsible for integrating tissue, is optimum in this case. Similarly, at a voltage of 160 V, the average thickness of the layer is 7 μm, with a slight decrease. The intermediate layer is predominant. The deep structure of the sample was not affected in this case. Further, for the sample anodized at 200 V, the average thickness of the oxide layer is 6.3 μm. The inner part has the major contribution in its

formation, and the metal was not affected at larger depths (figure 3 h). Finally, for the sample anodized at 250 V (figure 3i), the average thickness of the layer records the maximum value of 12.6 μm. The external layer plays a major role in its formation, containing mainly titanium oxide-embedded electrolyte. Because the inner layer has a small thickness, it is likely that the adhesion of the oxide layer is very poor. Even if, theoretically, under these anodizing conditions, good tissue integration could be achieved, the solution is not recommended in the case of the implants exposed to high mechanical stress. The metal structure is not affected at larger depths.

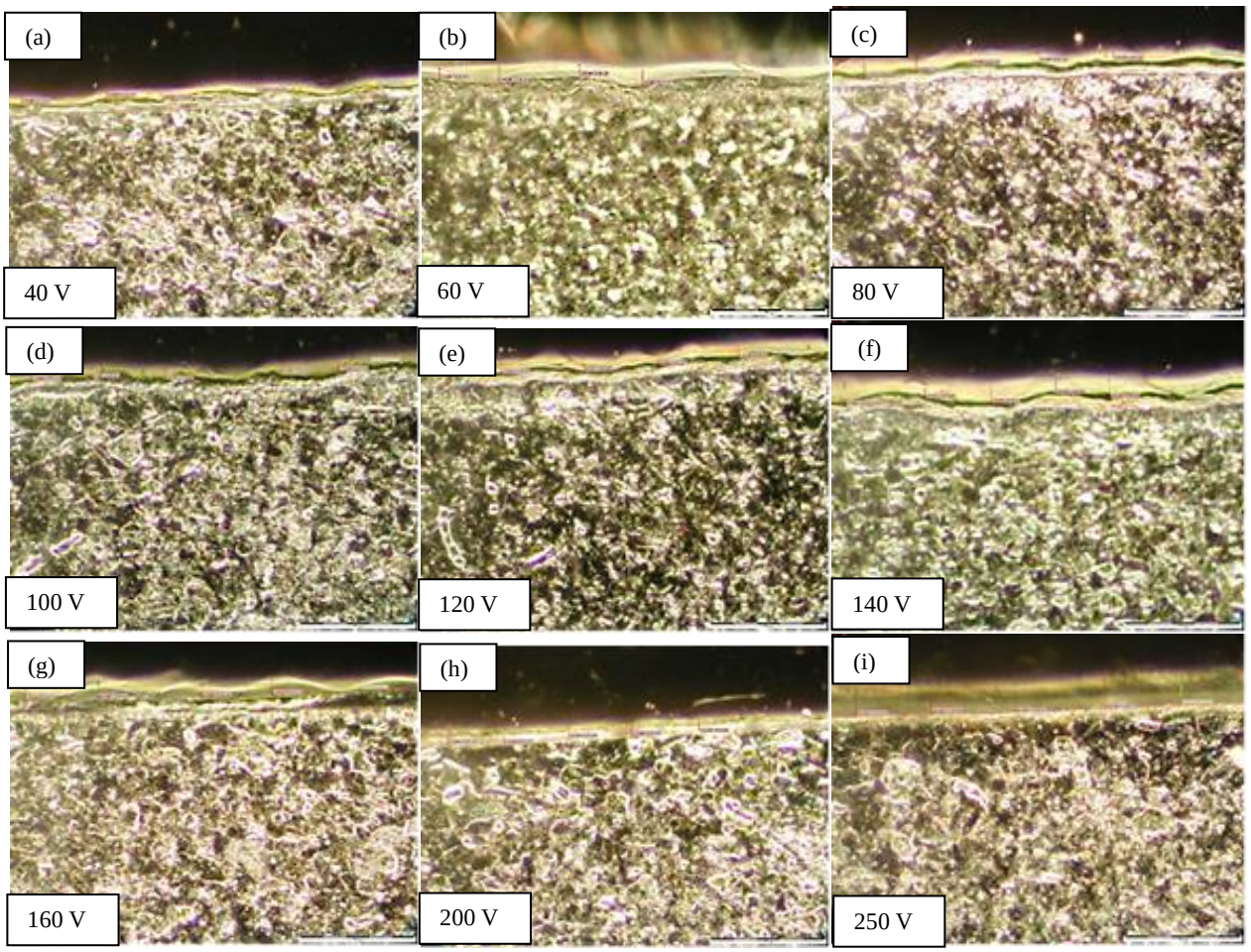

Figure 3 a-i. Layer thicknesses for the samples anodized at 40 V to 250 V; dark-field optical microscopy, magnification = 500 ×.

For all samples analysed, the anodizing process is considered to not affect the material at larger depths. The top layer is continuous and adherent, and its surface form confirms the issues highlighted above in the analysis of the sample surface. The average thickness of the anodized layers determined using the software and digital imaging microscopic Analysis FiveDocu are presented in Table 2.

Table 2. Average thickness of the anodized layers.

Number of sample	Thickness [μm]
1 (40 V)	3.1
2 (60 V)	6
3 (80 V)	6.1
4 (100 V)	5
5 (120 V)	6
6 (140 V)	8.5
7 (160 V)	7
8 (200 V)	6.3
9 (250 V)	12.6

The layer thickness of TiO_2 is well known to be strongly dependent on the experimental conditions. H.Z. Abdullah et al. reported layer thicknesses of just up to 3 μm obtained in H_2SO_4 containing H_2O_2 and/or H_3PO_4 at anodizing voltages between 90 and 180 V for times in the range 1 – 50 min [19]. Likewise, L. Wu et al. realized anodic oxide films on titanium alloy in 0.2 M sodium tartrate solutions, obtaining oxide thicknesses of approximately 4 μm in 30 min at increasing voltage up to 100 V [20]. Thicker films (up to 19 μm) were obtained by A. Karambakhsh et al. in sulphuric acid (anodizing time: 30 s, voltage: 80 V) [21].

3.3. Corrosion tests

The study of the corrosion behaviour was performed in accordance with SR EN ISO / IEC 10725:2005. The method is based on the direct correlation among the corrosion potential *E(i=0)*, the corrosion current I_{corr}, the polarization resistance R_p, and the electrical quantities measured between the electrodes. Some of the resulting voltammograms and Tafel slopes are shown in figures 4, a-d. The experimental values obtained in all corrosion tests are presented in Table 3.

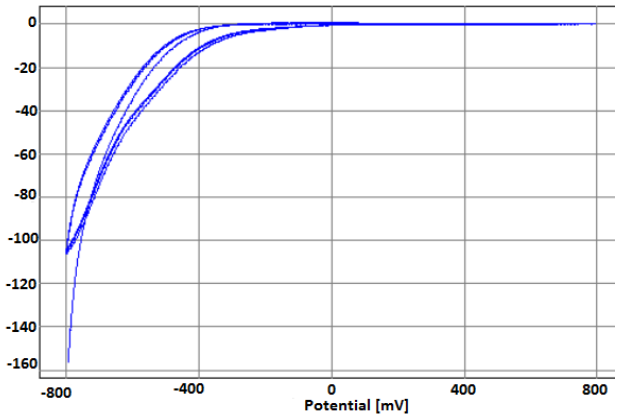

A

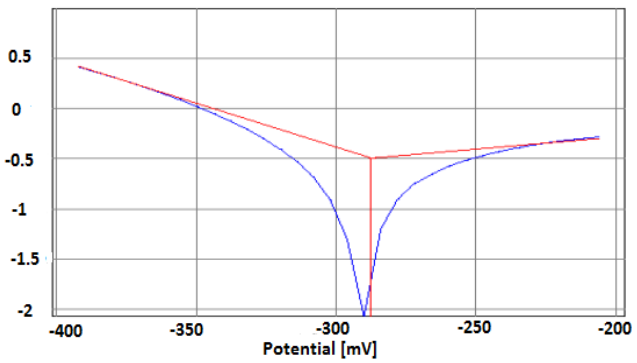

c

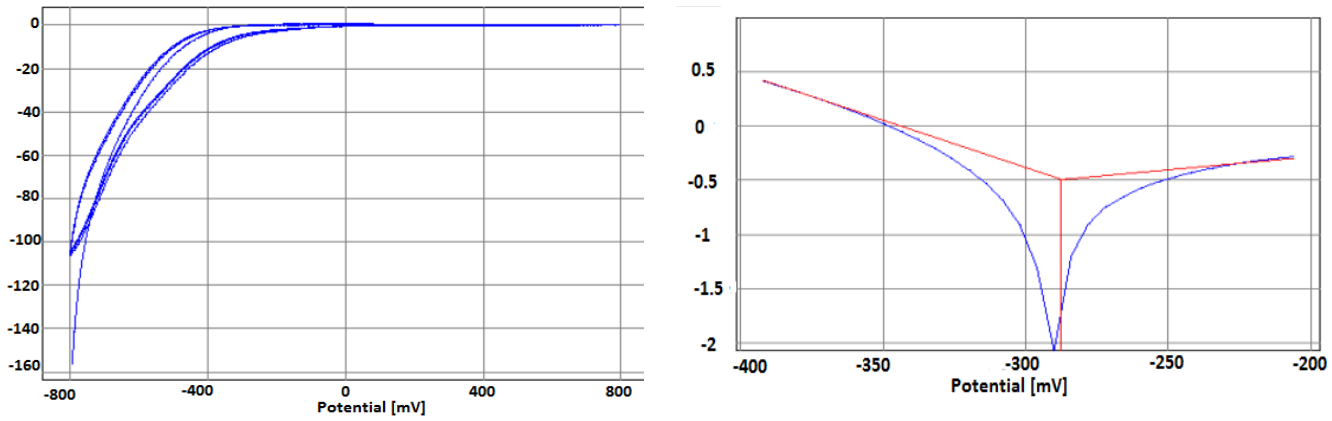

B **d**

Figure 4. Voltammograms on Ti at 40 V (a) and 200 V (b) and corrosion Tafel slopes at 40 V (c) and 200 V (d).

Table 3. Experimental results for the corrosion rate:

Voltage [V]	Corr. rate [μm/year]	$E_{(i=0)}$ [mV]	*I corr* [μA/cm²]	*Rp* [kohm·cm²]
40	2.8	-287	0.320	117
60	2.7	-453	0.312	17.5
80	1.85	-344	0.213	103
100	1.68	-282	0.193	349
120	1.67	-367	0.192	64
140	1.61	-354	0.185	100
160	1.46	-399	0.168	126
200	1.46	-366	0.167	76
250	1.17	-331	0.134	79

The corrosion rate values obtained in Ringer lactate solution are very low, and a good correlation is found between the TiO_2 thickness and the corrosion rate of the samples, expressed in μm $year^{-1}$ or as a corrosion current, in μA cm^{-2}. As expected, the polarization resistance in Ringer solution is much higher than those reported by J. Liu et al. for TiO_2 in a diluted sulphuric acid solution containing chloride ions [22].

3.4. Surface roughness

Figures 5 a – d show the D profiles of the control sample (figure 4a), the sample anodized at 40 V, (figure 4b), the sample anodized at 140 V (figure 4c), and the sample anodized at 200 V (figure 4d). The average roughness *Ra* is the arithmetic average of the absolute values of the roughness profile ordinates. The experimental measurements were made on seven standard reference lengths (7 × 0.8 mm = 5.6 mm). The roughness parameters were determined according to DIN ISO 1302:2002(E) and DIN EN ISO 11562:1998 standards [23, 24].

Systematic collection of data from the anodized samples highlights how anodization affects three important aspects of the implants behaviour: the oxide thickness, the corrosion rate and the surface roughness. Increasing the value of the applied potential (Table 4) corresponds to an increase of the thickness of the oxide layer on the surface of the implant, together with a corresponding decrease in the rate of corrosion. By graphically reproducing the simultaneous variation of the designated parameters, it can be concluded that the best voltage range for anodizing is 100 V – 150 V. This observation is confirmed by studies of cell adhesion, which records an optimum for the same range.

A simple statistical test of correlation reveals a strong positive linear relationship between the layer thickness and Ra, with a correlation factor r = 0.858 (figure 5a), and a weak negative relationship between the corrosion rate and Ra, with a correlation factor r = -0.447 (figure 5b).

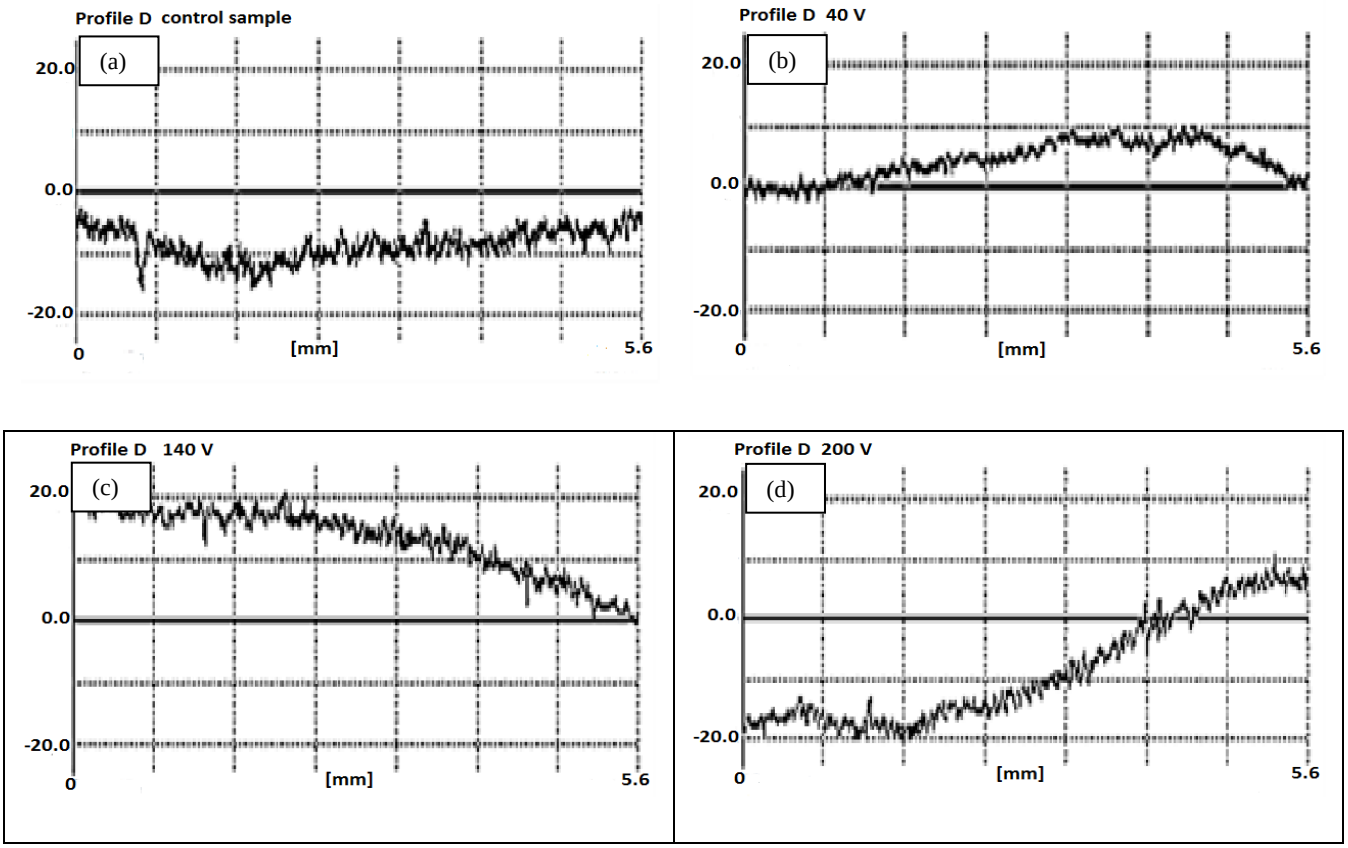

Figure 5 a – d. D profiles for some samples.

Table 4. Experimental data processing.

Voltage [V]	Corr. Rate [µm/year]	Layer thickness [µm]	Ra [µm]
40	2.8	3.11	0.575
60	2.7	6	0.609
80	1.9	6.1	0.539
100	1.7	5	0.532
120	1.7	6	0.459
140	1.6	8.5	0.869
160	1.5	7	0.617
200	1.5	6.3	0.664
250	1.2	12.6	0.998

Figure 6 shows the variation of the corrosion rate and oxide layer thickness according to the applied voltage. Because the corrosion rate and Ra can be considered the most important parameters, the reporting is based on these parameters.

The values obtained for the corrosion rate are comparable with those obtained by other authors for Ti surgical implants under similar working conditions, i.e., simulated body fluids (SBF) at 37°C [25, 26, 27].

Examining the graph, it can be concluded that the optimum anodization is for an applied potential in the range of 100 V - 150 V. This result is confirmed by the evidence of cell adhesion, which presents an optimum for the same range.

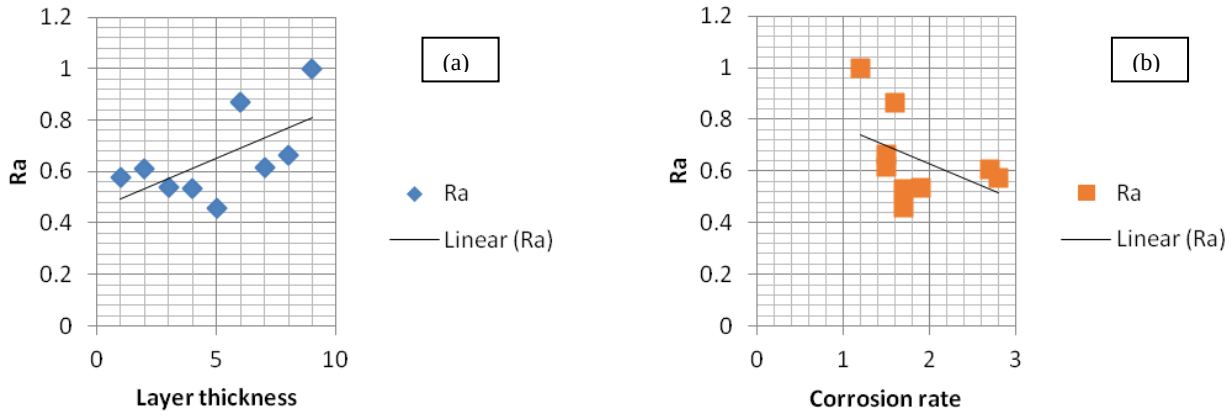

Figure 5 a and b. Statistical correlations between Ra and the layer thickness (a) or the corrosion rate (b).

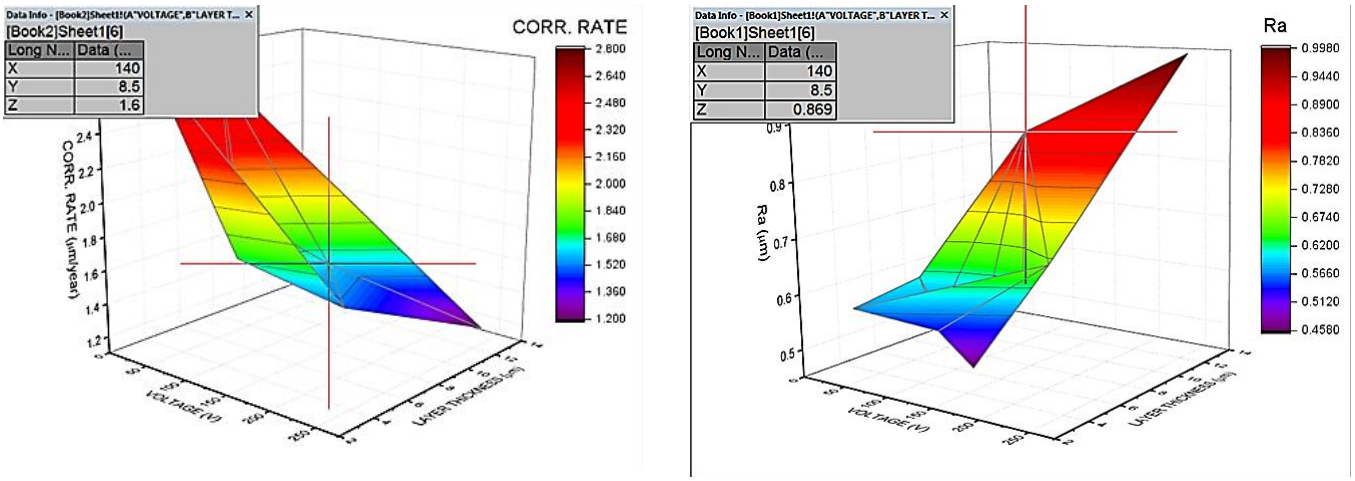

Figure 6. Interdependency of the studied parameters.

The Ra values for the anodized samples are higher than those obtained for the control sample (titanium plate, being only chemically polished in the same way as the rest of the sample) and are sufficiently large for the anodized sample at 140 V (Ra = 0.849 μm and corrosion rate = 1.6 μm/year),

which confirms the observation that the anodization results are optimal for applied potentials around this value.

3.5. Cell adhesion

To test the degree of adhesion of MSCs on the previously anodized Ti surfaces, mesenchymal cells obtained from bone marrow were used. These cells were collected via aspiration from the posterior-upper iliac crest or from the front face of the sternum. [10, 28, 29]. The cells obtained this way were trypsinized with Trypsin-EDTA, counted, dosed, and then incubated in the culture media in which plates of Ti and witness samples were also introduced.

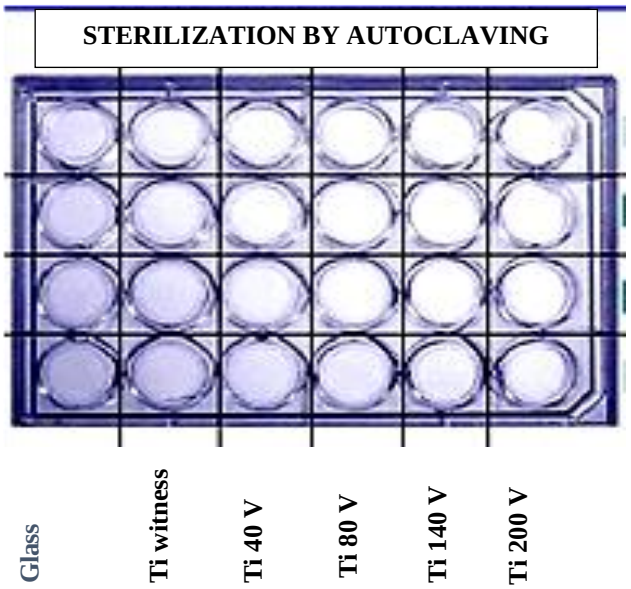

Figure 7. Placement of the materials in the wells.

Table 5. Cellular adherence.

Sample	Number of cells adhered on surface
Glass	45000
Ti witness	30000
40 V	45000
80 V	60000
140 V	80000
200 V	65000

The Flow Cytometry technique and monoclonal antibody combinations were used for identification and quantification of the MSCs. Monoclonal antibodies used in the Flow Cytometry are

coupled with specific dyes (fluorochromes). The most commonly used fluorochromes are fluorescein isothiocyanate (FITC) and phycoeritrina (PE).

The protocol used for cellular adherence testing contains the following steps:

1. Materials sterilization by autoclaving 8 pieces of any material.
2. Placing the materials in wheels.
3. In all the wheels, 100000 cells / 30 μL/ wheel are introduced, as counted using flow cytometry. We used the standard method of cell counting in a Neubauer chamber.
4. The plates are incubated for 1 hour at 37 °C.
5. Next, each wheel is completed with 1.5 mL of incubation environment - foetal bovine serum (FBS) + Fibroblast Growth Factor (FGF), 2 ng/mL.
6. After 24 h, the plate is read (figure 7):
   a. The supernatant is aspirated.
   b. By the method mentioned above, the MSC in suspension are counted again, with the difference determining the number of cells adhered on the surface of Ti samples or witnesses.

The arrangement of the materials in the wells is shown in figure 7. The obtained results are presented in table 5.

Studies have shown that in the present case, the applied surfaces modifications treatments for the anodized titanium surface produces a maximal adhesion at a voltage value of approximately 150 V (figure 8).

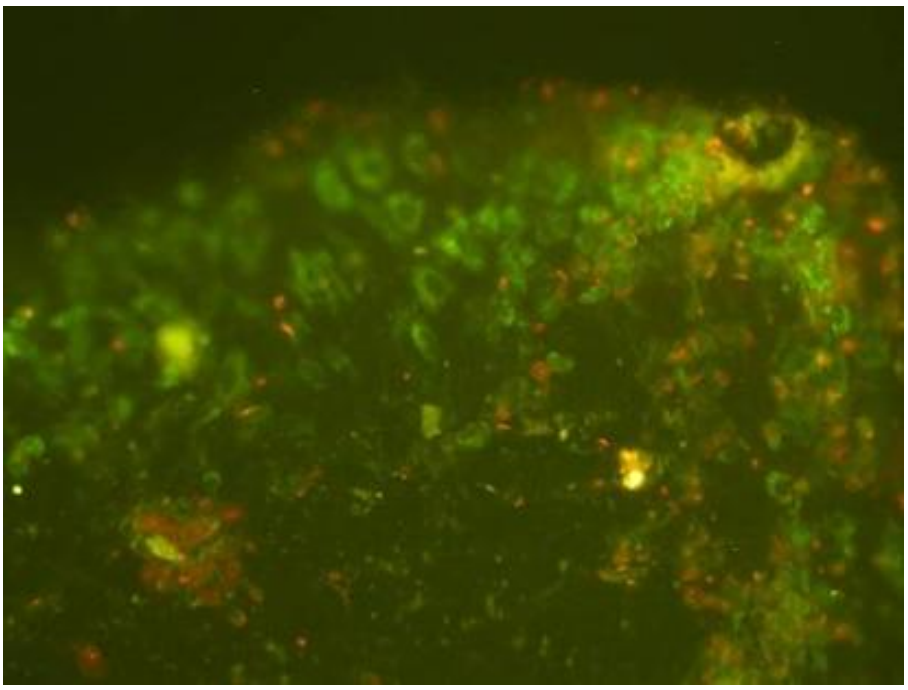

Figure 8. Cell adhesion onto the surface anodized at 150 V; OM fluorescence, dyed with FITC.

4. CONCLUSIONS

1. This study proved than surface texture, layers thickness, roughness, corrosion rate and other surface characteristics of a biomedical implant can significantly influence the interaction of implants with the surrounding biological / biochemical environment.

2. Experimental determination of the corrosion rates of the anodized samples in Ringer lactate solution revealed that as a result of analysing the experimental data, the optimal range of anodization is 100-150 V for medical applications. The result was confirmed by the cell adhesion evidence, which yielded an optimum for the same interval of anodizing voltage.

3. The study opens the achievement of functionalized surfaces for titanium implants, enabling better integration both at the systemic level (by reducing the quantity of metal ion released due to corrosion) and at the cellular level. At the cellular level, the functionalization of implants' surface and better adhesion degree, particularly for embryonic stem cells, enables populating the implant surface with cells capable of differentiating and specializing, thereby ensuring total body integration and, by default, a better functional recovery.

References

1. F. El-Taib Heakal, O.S. Shehata, N. S. Tantawy, *Int. J. Electrochem. Sci.,* 9 (2014) 1986–2004.
2. A.M. Fekry, M.A. Ameer *Int. J. Electrochem. Sci*., 6 (2011) 1342 – 1354.
3. N. A. Al-Mobarak, A. A. Al-Swayih, *Int. J. Electrochem. Sci*., 9 (2014) 32– 5.
4. K. Das, S. Bose, A. Bandyopadhyay, *Acta Biomaterialia,* 3 (2007) 573–585.
5. M. Songur, H. Celikkan, F. Gokmese, S. A. Simsek, M. L. Aksu, *J. Appl. Electrochem.,* 39 (2009) 1259–1265.
6. M. P. Neupane, I. S. Park, S. J. Lee, K. A. Kim, M. H. Lee, T. S. Bae, *Int. J. Electrochem. Sci.,* 4 (2009) 197–207.
7. F. El-Taib Heakal, O.S. Shehata, N.S. Tantawy, *Int. J. Electrochem. Sci.,* 9 (2014) 1986 – 2004.
8. L-H. Lia, Y-M. Konga, H-W. Kima, Y-W. Kima, H-E. Kima, S-J. Heob, *Biomaterials,* 25, Issue 14, June 2004, Pages 2867–2875.
9. A. Karambakhsh, A. Afshar, S. Ghahramani, P. Malekinejad, *JMEPEG*, 20(2011) 1690–1696.
10. L. Wu, J. Liu, M. Yu, S. Li, H. Liang, M. Zhu, *Int. J. Electrochem. Sci.,* 9 (2014) 5012 – 5024.
11. J. Xing, Z. Xia, Y. Zhang, L. Zhong, *Int. J. Electrochem. Sci.,* 7 (2012) 12808 – 12816.
12. A. Ghiban, P. Moldovan, *U.P.B. Sci. Bull. Series B,* 74 (2012), 203-214.
13. M. Popa, C. Vasilescu, S. I. Drob, J. M. Calderon Moreno, *Int. J. Electrochem. Sci.,* 8 (2013) 5287–5298.
14. ASTM F86-04: Standard Practice for Surface Preparation and Marking of Metallic Surgical Implants.
15. Y. J. Liu, J. Y. Xu, W. Lin, C. Gao, J. C. Zhang, X. H. Chen, *Rev. Adv. Mater. Sci.,* 3 (2013) 126-130.
16. L. Liu, P. Yang, C. Su, H. Guo, M. Z. An, *Int. J. Electrochem. Sci.,* 8 (2013) 6077 – 6084.
17. M. Iwasaki, K. Shimada, K. Kudo, Y. Tamagawa, H. Horikawa, *Materials Transactions,* 52 (2011) 1410-1417.
18. M. M. Dicu, M. Abrudeanu, J-P. Millet, S. Moga, V. Rizea, C. Ducu, *U.P.B. Sci. Bull., Series B,* 74 (2012) 193-202.
19. H. Z. Abdullah, C. C. Sorrell, *J. Aust. Ceram. Soc.*, 43 (2007) 125-130.
20. L. Wu, J. Liu, M. Yu, S. Li, H. Liang, M. Zhu, *Int. J. Electrochem. Sci.,* 9 (2014) 5012 – 5024.

21. A. Karambakhsh, A. Afshar, S. Ghahramani, P. Malekinejad, *J. Mater. Eng. Perform.*, 20 (2011) 1690 –1696.
22. J. Liu, A. Alfantazi, E. Asselin, *Appl. Surf. Sci.*, 332 (2015) 480–487.
23. DIN ISO 1302:2002 (E).
24. DIN EN ISO 11562:1998.
25. W. Aperador, J.C. Caicedo, R. Vera, *Int. J. Electrochem. Sci.*, 8 (2013) 2778 – 2790.
26. D. M. Gordin, T. Gloriant, V. Chane-Pane, D. Busardo, V. Mitran, D. Hoche, C. Vasilescu, S. I. Drob, A. Cimpean, *J. Mater. Sci: Mater. Med.*, 23 (2012) 2953–2966.
27. C.Y. Zheng, F.L. Nie, Y.F. Zheng, Y. Cheng, S.C. Wei, R.Z. Valiev, *Appl. Surf. Sci.*, 257 (2011) 5634–5640.
28. S. Lavenus, M. Berreur, V. Trichet, P. Pilet, G. Louarn, P. Layrolle, *European Cells and Materials* 22(2011) 84-96.
29. D. B. S Mendonca, P.A. Miguez, G. Mendonca, G. Mendonça, M. Yamauchi, F. J. L. Aragão, L. F. Cooper, *Bone,* 49 (2011) 463-472.